

Runaway electron beam initiated by capacitive discharge plasma at the air pressure of 0.4 and 1 Torr

© E.Kh. Baksht, V.F. Tarasenko, N.P. Vinogradov

Institute of High Current Electronics, Russian Academy of Sciences, Siberian Branch, Tomsk, Russia
E-mail: VFT@loi.hcei.tsc.ru

Received October 15, 2024

Revised November 14, 2024

Accepted November 15, 2024

During the formation of plasma diffuse jets initiated by plasma of a capacitive discharge in low pressure air, a runaway electron beam (REB) was detected with a collector. It was found that REB gets ahead of the front of the plasma diffuse jet. The REB current amplitude in the pulse periodic mode was shown to increase with increasing pulse repetition rate.

Keywords: runaway electron beam, low pressure air, capacitive discharge, plasma diffuse jets.

DOI: 10.61011/TPL.2025.03.60728.20152

Over the last thirty years, much attention has been paid to studying atmospheric discharges in the stratosphere and mesosphere, which are distinguished by a great variety of forms [1,2]. Among the varieties of these discharges there are columnar red sprites (CRSs) whose photographs are given in many papers (e.g. [3,4]). CRSs are initiated at the altitude of about 75 km above sea level and first propagate to the Earth surface. Authors of [5,6] suggested that formation of high altitude atmospheric discharges is significantly affected by runaway electrons (REs). The existence of intense X-ray and gamma radiation from atmospheric discharges at the altitudes of 30 km and lower was revealed in [7] and confirmed in many publications (e.g. [8,9]). However, results of direct measurements of bremsstrahlung X-ray and gamma radiation or RE beams inducing this radiation from CRS plasma are still unavailable. It is quite difficult to detect the runaway electron beams and bremsstrahlung X-ray radiation while they interact with air particles during high altitude discharges. In particular, this is caused by instability of the time and place of the red sprites emergence and also by the presence of X-ray and gamma radiation from lightning discharges at lower altitudes [7–10].

Note that in a number of studies (e.g. [11–13]) X-ray radiation and runaway electron beam (REB) have been detected during nanosecond discharges in long tubes filled with low pressure gases, including air, when high voltage pulses were applied. However, in those studies REs were initiated by plasma contacting with the metal cathode, and the discharge color was not compared with that of CRSs.

In our previous papers [14–16] we described red colored plasma diffuse jets (PDJs) that are laboratory analogues of CRSs. PDJs consisted of streamers [16] and had emission spectra and plasma parameters similar to those detected for CRSs. In addition, PDJs were initiated by the plasma of a pulse periodic capacitive discharge not contacting metal electrodes.

The goal of this paper is to demonstrate that in a capacitive pulse periodic discharge in low pressure air REBs may be generated from plasma that has no contact with metal electrodes.

The studies were carried out on a modernized setup that we used in [14–16] to examine the PDJ properties. In this work, the REB current was measured by a collector mounted on the quartz tube right end and allowing direct detection of REBs. In addition, a high voltage generator was used. The setup schematic diagram and photograph of its main part are given in Figs. 1, *a* and *b*.

PDJs were formed by applying negative polarity voltage pulses from generator NPG-18/3500N whose transmission line resistance was 75Ω ; the amplitude of those pulses in the incident wave was 12–18 kV at the half-height duration of ~ 6 ns and front duration of ~ 3 ns. The pulse repetition rate f was 8.6, 62 or 1980 Hz. The voltage pulses were delivered to electrodes 2 and 3 mounted 6 cm apart via a cable 3.85 m long. The generator high-voltage terminal was connected either to electrode 3 (Figs. 1, *a* and *c*) or to electrode 2 (Fig. 1, *b*). In a number of experiments, a matching resistance of 75Ω was connected to electrodes 2–3. This allowed reduction of electromagnetic interference and detection of the discharge current, but halved the voltage applied to electrodes 2–3. In addition, the matching resistance prevented formation of the second voltage pulse due to reflections from the gap between electrodes 2–3 and generator. The quartz tube was filled with laboratory air with relative humidity of $\sim 43\%$. The main measurements were performed at the temperature of $\sim 25^\circ\text{C}$ and pressures of 0.4 or 1 Torr.

Voltage between the high-voltage and grounded ring electrodes was measured by using probe TT-HVP 2739 with the bandwidth of 220 MHz. Discharge current in the circuit of the generator and capacitive discharge plasma was measured by a shunt 0.1Ω in resistance, which was assembled from resistors TVO. The discharge

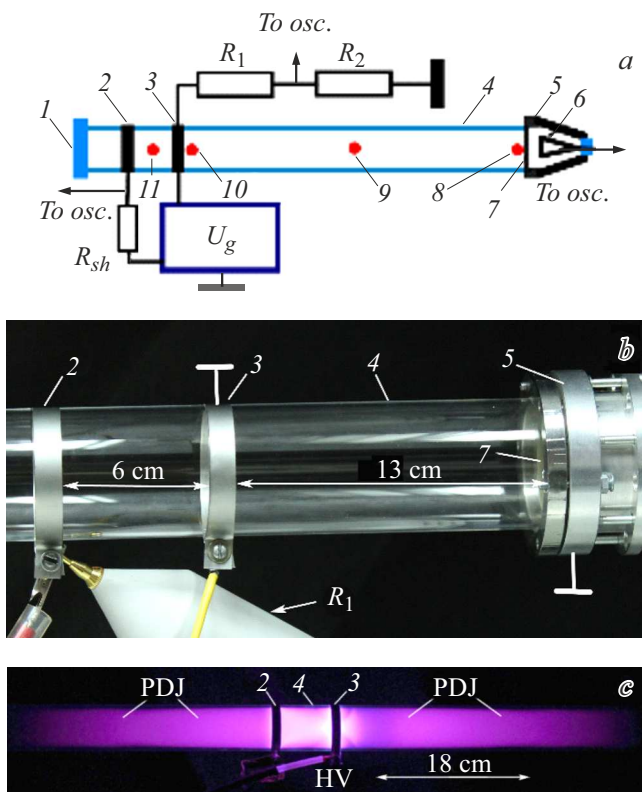


Figure 1. *a* — setup schematic diagram; *b* — photograph of the setup main part; *c* — photograph of the discharge glow in the 100 cm long quartz tube with electrodes located in its central part. 1 — left end caprolon flange, 2 and 3 — external ring electrodes 1 cm wide made of foil 100 μm thick, 4 — quartz tube with internal diameter of 5 cm and wall thickness of 2.5 mm, 5 — collector body, 6 — collector receiver 2 cm in diameter, 7 — nickel grid 140 μm thick, light transparency of $\sim 20\%$, cell size of no more than $70 \times 70 \mu\text{m}$ (to ensure screening of the dynamic capacitive current [18]), 8–11 — discharge regions where from radiation was fed through the lightguide to silicon photomultiplier (SiPM). R_1 and R_2 — resistors of voltage divider TT-HVP 2739, R_{sh} — shunt resistance of 0.1 Ω , U_g — negative polarity pulse generator NPG-18/2000N. PDJ — plasma diffusion jets.

photos were taken with camera Canon 2000D. Emission spectra in the range of 200–1000 nm were recorded with spectrometer HR2000+ES (range of 200–1150 nm, optical resolution of ~ 0.9 nm) having the known spectral sensitivity. The radiation temporal characteristics were determined by a silicon photomultiplier (SiPM) (included in the MicroFC-SMA-10035 module) with the transient response rise time of 0.3 ns. The beam current pulses were measured by a collector with the time resolution of ~ 100 ps [17]. Electrical signals from the divider, shunt, collector and SiPM were fed to oscilloscope Tektronix MDO 3104 (1 GHz, sampling rate 5 GS/s). The discharge was photographed in the absence of external lighting.

The measurements performed confirmed that voltage pulses applied to the external ring electrodes form in the tube plasma diffuse jets propagating in both directions

from the area of their initiation (Fig. 1, *c*). The PDJ length increased with decreasing pressure, as well as with increasing voltage pulse amplitude. When generator NPG-18/2000N was used, the jet color changed some what relative to that of PDJ in the case of generator G2 which generated voltage pulses ~ 7 kV in amplitude at the half-height duration of $\sim 2 \mu\text{s}$ and front duration of 350 ns [14]. As the pressure increased, the discharge color acquired a blue tint, which was caused by enhancement of the contribution of the second positive (2+) and first negative (1-) systems of the nitrogen molecule and ion bands, respectively. Red color of the discharge plasma radiation was determined by the bands of the first positive system (1+) of the nitrogen molecule. The PDJ length at the air pressures of 0.4 and 1 Torr was significantly greater than the distance (13 cm) from the right edge of ring electrode 3 to the collector grid 7; in the experiments on measuring REBs, their glow front reached both quartz tube ends.

In the case of generator NPG-18/3500N, the RE beam was detected in wide ranges of air pressures and voltages at electrodes 2–3. The beam amplitude increased with increasing frequency f . Fig. 2 presents the pulses of REB, voltages in the gap, and discharge current from the shunt.

The runaway electron beam was measured with the total detection time resolution no worse than 0.9 ns. The maximum current amplitude was measured with delay $\Delta t \approx 5.6$ ns relative to the maximum pulse voltage. This is associated with the time of flight of electrons from the nearelectrode region (where they gain most of their energy) to the collector. Variations in the position of the high-voltage electrode with respect to the collector did not affect the beam current generation. When the grounded ring electrode was located between the high-voltage electrode and grounded collector whose grid was 14 cm apart the grounded ring electrode, REB was also detected. This allowed a conclusion that fast electrons gain their main acceleration near the high-voltage ring electrode. When the 100 μm -thick paper filter was located behind the mesh, REB was not detected because of relatively low RE energy.

Average electron energy T was estimated using well-known formula $T = mv^2/2$ where m is the electron mass, v is the electron velocity. Average electron velocity $v_{av} = l/\Delta t$ (where the gap between the right edge of high-voltage electrode 2 and collector receiver is $l = 21$ cm and $\Delta t \approx 5.6$ ns) was 3.75 cm/ns. According to the data presented in Fig. 1 of [19], the extrapolated electron range in air at the energy of ~ 4 keV and air pressure of 1 Torr is 60 cm which is significantly greater than the distance from the high-voltage electrode edge to collector.

When generator G2 with the pulse front duration of ~ 350 ns and ring electrode voltage of ~ 7 kV was used, the runaway electron beam was not detected.

The PDJ propagation speed was determined using SiPM to which radiation from the quartz tube was fed through a lightguide. Fig. 1, *a* shows regions 8–11 wherefrom PDJ radiation was detected; Fig. 2, *b* presents the oscillograms of

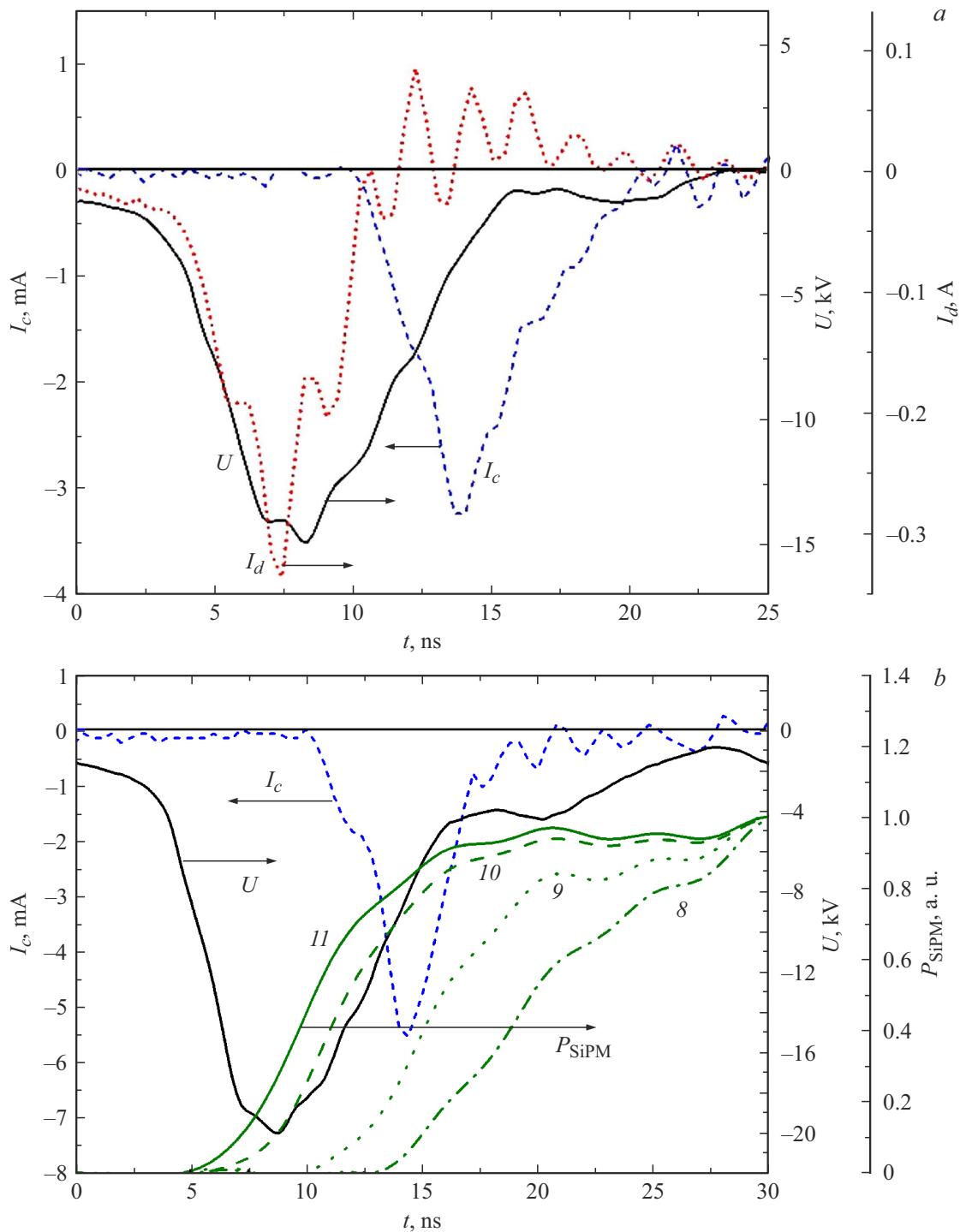


Figure 2. *a* — oscillograms of pulses of voltage U , discharge current I_d and beam current I_c at $p = 0.4$ Torr and $f = 1980$ Hz. *b* — oscillograms of U , I_c and optical signal P_{SiPM} from regions 8–11 (Fig. 1, *a*) at $p = 1$ Torr and $f = 62$ Hz. REB amplitude in panel *b* is greater at a lower frequency and higher pressure than that in panel *a* because of an increase in voltage at electrodes 2–3 in the absence of matching resistance.

radiation pulses from these regions; the pulse intensities are normalized to unity. Diameter of the region of radiation getting to the end of the lightguide located at different distances from the end of the ring electrodes at the same distance to the tube surface was ~ 1 cm. Fig. 3 presents average speeds

of the PDJ glow front propagation along the tube towards the collector for different regions.

The highest speed was observed near the electrodes in region A. As the pressure decreased, the ionization wave front velocity increased. It was found out that at

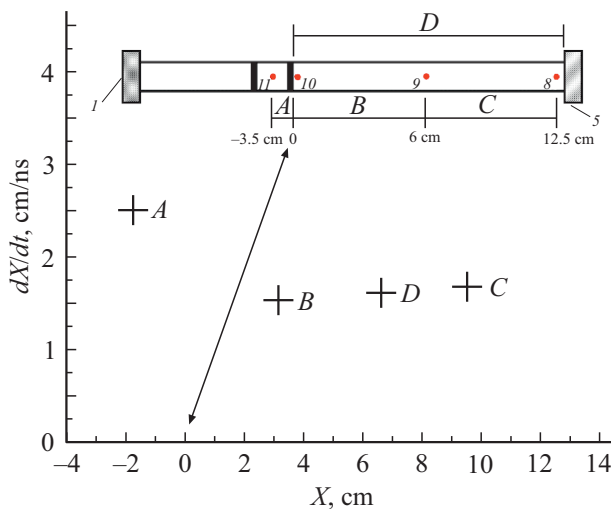


Figure 3. Average propagation speeds of the PDJ glow front at the level of 0.5 towards the collector in the intervals between regions 11–10 (A), 10–9 (B), 9–8 (C) and 10–8 (D) in Fig. 1, a at $p = 1$ Torr and $f = 62$ Hz. X -coordinates of the curve points correspond to those of midpoints indicated in the inset.

$p = 0.4$ Torr the plasma glow at the collector end in region 8 appeared earlier than in the middle of the tube; this may be explained by the counter streamer initiation in region 9 by runaway electrons and bremsstrahlung X-ray radiation from the collector under the REB impact. At $p = 1$ Torr, the runaway electron beam also arrived at the collector earlier than the PDJ front (Fig. 2, b) but had no time to initiate at the collector a considerable reverse streamer.

The results presented show that, when the air pressure is 1 Torr and less, the runaway electron beam is generated simultaneously with the PDJ formation from plasma created by the pulse periodic capacitive discharge. The REB amplitude increased with increasing generator voltage and, taking into account the grid transparency, exceeded 25 mA at the collector receiver diameter of 2 cm. The half-height duration of the beam current pulse at the air pressure of 1 Torr was ~ 3 ns, while its highest density was ~ 8 A/cm². The experiments have shown that REs gain the main energy in the vicinity of electrodes where the strongest electric field is observed. Runaway electrons may be assumed to play a significant role in the formation of negative streamers in red sprites; REs are accelerated in the regions of the maximum reduced electric field during initiation of streamers and affect the red sprite shape.

The studies conducted have shown that, when plasma diffuse jets are formed by a pulse-periodic capacitive discharge, REB is generated in the absence of contact between the initiating plasma and metal cathode. It has been established that under these conditions REB gets ahead of the PDJ front and is detected by the collector prior to the PDJ arrival. These results may be used in investigating high-altitude discharges.

Funding

The study was supported by the Russian Science Foundation (Project № 24-29-00166).

Conflict of interests

The authors declare that they have no conflict of interests.

References

- [1] V.P. Pasko, *J. Geophys. Res.*, **115**, A00E35 (2010). DOI: 10.1029/2009JA014860
- [2] V.V. Surkov, M. Hayakawa, *Surv. Geophys.*, **41** (5), 1101 (2020). DOI: 10.1007/s10712-020-09597-3
- [3] J. Qin, S. Celestin, V.P. Pasko, S.A. Cummer, M.G. McHarg, H.C. Stenbaek-Nielsen, *Geophys. Res. Lett.*, **40** (17), 4777 (2013). DOI: 10.1002/grl.50910
- [4] R. Marskar, *Plasma Sources Sci. Technol.*, **33**, 025024 (2024). DOI: 10.1088/1361-6595/ad29c0
- [5] V. Yukhimuk, R.A. Roussel-Dupré, E.M.D. Symbalysty, Y. Taranenko, *J. Geophys. Res. Atmos.*, **103** (D10), 11473 (1998). DOI: 10.1029/98JD00348
- [6] A.V. Gurevich, K.P. Zybin, Y.V. Medvedev, *Phys. Lett., A*, **361** (1-2), 119 (2007). DOI: 10.1016/j.physleta.2006.05.063
- [7] G.J. Fishman, P.N. Bhat, R. Mallozzi, J.M. Horack, T. Koshut, C. Kouveliotou, G.N. Pendleton, C.A. Meegan, R.B. Wilson, W.S. Paciesas, S.J. Goodman, H.J. Christian, *Science*, **264** (5163), 1313 (1994). DOI: 10.1126/science.264.5163.1313
- [8] J.R. Dwyer, N. Liu, J.E. Grove, H. Rassoul, D.M. Smith, *J. Geophys. Res. Space Phys.*, **122** (8), 8915 (2017). DOI: 10.1002/2017JA024141
- [9] T. Neubert, N. Østgaard, V. Reglero, O. Chanrion, M. Heumesser, K. Dimitriadou, F. Christiansen, C. Budtz-Jørgensen, I. Kuvvetli, C.J. Eyles, *Science*, **367** (6474), 183 (2020). DOI: 10.1126/science.aax3872
- [10] R.J. Nemiroff, J.T. Bonnell, J.P. Norris, *J. Geophys. Res. Space Phys.*, **102** (A5), 9659 (1997). DOI: 10.1029/96JA03107
- [11] L.M. Vasilyak, S.V. Kostyuchenko, N.N. Kudryatsev, I.V. Filyugin, *Phys. Usp.*, **37** (3), 247 (1994). DOI: 10.1070/PU1994v037n03ABEH000011.
- [12] Y.Z. Ionikh, *Plasma Phys. Rep.*, **46**, 1015 (2020). DOI: 10.1134/S1063780X20100049
- [13] B. Huang, C. Zhang, J. Qiu, X. Zhang, Y. Ding, T. Shao, *Plasma Sources Sci. Technol.*, **28** (9), 095001 (2019). DOI: 10.1088/1361-6595/ab3939
- [14] V.F. Tarasenko, N.P. Vinogradov, E.Kh. Baksht, D.A. Sorokin, *J. Atmos. Sci. Res.*, **5**, 26 (2022). DOI: 10.30564/jasr.v5i3.4858
- [15] D.A. Sorokin, V.F. Tarasenko, E.Kh. Baksht, N.P. Vinogradov, *Phys. Plasmas*, **30** (8), 083515 (2023). DOI: 10.1063/5.0153509
- [16] V.F. Tarasenko, E.K. Baksht, V.A. Panarin, N.P. Vinogradov, *Plasma Phys. Rep.*, **49** (6), 786 (2023). DOI: 10.1134/S1063780X23700393
- [17] V.F. Tarasenko, D.V. Rybka, *High Voltage*, **1** (1), 43 (2016). DOI: 10.1049/hve.2016.0007

- [18] T. Shao, V.F. Tarasenko, C. Zhang, A.G. Burachenko, D.V. Rybka, I.D. Kostyrya, M.I. Lomaev, E.Kh. Baksht, P. Yan, *Rev. Sci. Instrum.*, **84**, 053506 (2013).
DOI: 10.1063/1.4807154
- [19] J.A. Gledhill, *J. Phys. A*, **6** (9), 1420 (1973).

Translated by EgoTranslating